E&MT
ENGINEERING & MATERIALS TECHNOLOGY DEPARTMENT

WSRC-TR-94-0357

Keywords: DWPF
Melter Feed
Rheology

Retention: Permanent

Recommendations for Rheological Testing and Modelling of DWPF Melter Feed Slurries(U)

Technical Assistance Request Number:
94-DWPT-PMC-A0003

By

M. A. Shadday Jr.

ISSUED: August 1994

Authorized Derivative Classifier

SRTC **SAVANNAH RIVER TECHNOLOGY CENTER, AIKEN, SC 29808**
Westinghouse Savannah River Company
Prepared for the U. S. Department of Energy under
Contract DE-AC09-89SR18035

PROJECT:	**Defense Waste Storage**
DOCUMENT:	**WSRC-TR-94-0357**
TITLE:	**Recommendations for Rheological Testing and Modelling of DWPF Melter Feed Slurries(U)**
TASK NUMBER:	**94-DWPT-PMC-A0003**
TASK TITLE:	**DWPF Melter Feed System Analysis**

APPROVALS

R. A. Dimenna, Technical reviewer — Date: 8.4.94

J. R. Pelfrey, Manager (EM&SG) — Date: 8-8-94

M. R. Buckner, Manager (ATS) — Date: 8-8-94

DISCLAIMER

Table of Contents

Nomenclature

A	Area
D	Tube diameter
$\vec{F}$	Force vector
F_z	Axial component of force
He	Hedstrom number
K	Non-dimensional ratio that is used to calculate the transition Reynolds number
kg	Kilograms
L	Length
m	Meters
n	Yield/power fluid exponent
Q	Flow rate
r	Radial coordinate
r_o	Radius of slug flow region in pipe flow of a non-Newtonian fluid, or yield radius
R	Tube radius
Re	Reynolds number
Re_B	Bingham Reynolds number
Re_c	Critical Reynolds number for laminar/turbulent transition
s	Seconds
t	Time
V	Average velocity
$\vec{V}$	Velocity vector
v	Velocity
$\bar{v}$	Average velocity
v_r	Radial velocity component

v_z Axial velocity component

v_θ Azimuthal velocity component

α Non-dimensional yield radius

α_c Critical value of the non-dimensional yield radius

ΔP Axial pressure drop

$\dot{\gamma}$ Strain rate

ξ Non-dimensional radial coordinate

η_o Consistancy for a Bingham plastic or a yield/power law fluid

ρ Density

τ_{rz} Shear stress

τ_o Yield stress for a Bingham plastic or a yield/power law fluid

τ_ω Wall shear stress

τ_R Wall shear stress

Introduction and Summary

The melter feed in the DWPF process is a non-Newtonian slurry. In the melter feed system and the sampling system, this slurry is pumped at a wide range of flow rates through pipes of various diameters. Both laminar and turbulent flows are encountered. Good rheology models of the melter feed slurries are necessary for useful hydraulic models of the melter feed and sampling systems.

A concentric cylinder viscometer is presently used to characterize the stress/strain rate behavior of the melter feed slurries, and provide the data for developing rheology models of the fluids. The slurries exhibit yield stresses, and they are therefore modelled as Bingham plastics. The ranges of strain rates covered by the viscometer tests fall far short of the entire laminar flow range, and therefore hydraulic modelling applications of the present rheology models frequently require considerable extrapolation beyond the range of the data base. Since the rheology models are empirical, this cannot be done with confidence in the validity of the results. Axial pressure drop versus flow rate measurements in a straight pipe can easily fill in the rest of the laminar flow range with stress/strain rate data. The two types of viscometer tests would be complementary, with the concentric cylinder viscometer providing accurate data at low strain rates, near the yield point if one exists, and pipe flow tests providing data at high strain rates up to and including the transition to turbulence.

With data that covers the laminar flow range, useful rheological models can be developed. In the Bingham plastic model, linear behavior of the shear stress as a function of the strain rate is assumed once the yield stress is exceeded. Both shear thinning and shear thickening behavior have been observed in viscometer tests. Bingham plastic models cannot handle this non-linear behavior, but a slightly more complicated yield/power law model can. The flow rate versus pressure drop relation for a yield/power law fluid, analogous to the Buckingham-Reiner equation for a Bingham plastic (Bird, Stewart, & Lightfoot, 1960), has been derived, as have been relations for predicting the point of transition to turbulence. The predicted flow rate vs pressure drop behaviors of the two models, based on existing viscometer data, show significant differences between the predicted behaviors of the two models. Also the danger of extrapolating a rheological model beyond the range of the data base is illustrated. Only laminar pipe flow is considered, but that is because the impact of non-Newtonian effects is much greater for laminar pipe flow than it is for turbulent pipe flow. The primary objective of this document is to establish the need for viscometry data that covers the entire laminar flow range.

Rheology Models

The melter feed slurries are presently modelled as Bingham plastics, and the data to support these models is obtained with concentric cylinder viscometers. Figure 1 is typical plot of viscometer data for five different slurries (Marek, 1994). The slurries differ in the percent weight of total solids. The vertical ordinate of the plot is the shear stress, and the horizontal ordinate is the strain rate. For pipe flow, the strain rate is the absolute value of the radial velocity gradient.

The viscometer data show that the fluids exhibit yield stress type behavior, and they also clearly show non-linear behavior for non-zero strain rates. While the existance of a yield stress in fluids is controversial (Bird, Armstrong, & Hassager, 1987) it is a useful concept for modelling the behavior of some non-Newtonian fluids. The bottom three rheograms

in figure 1 exhibit shear thinning or pseudoplastic behavior, and the top two rheograms exhibit shear thickening or dilatant behavior.

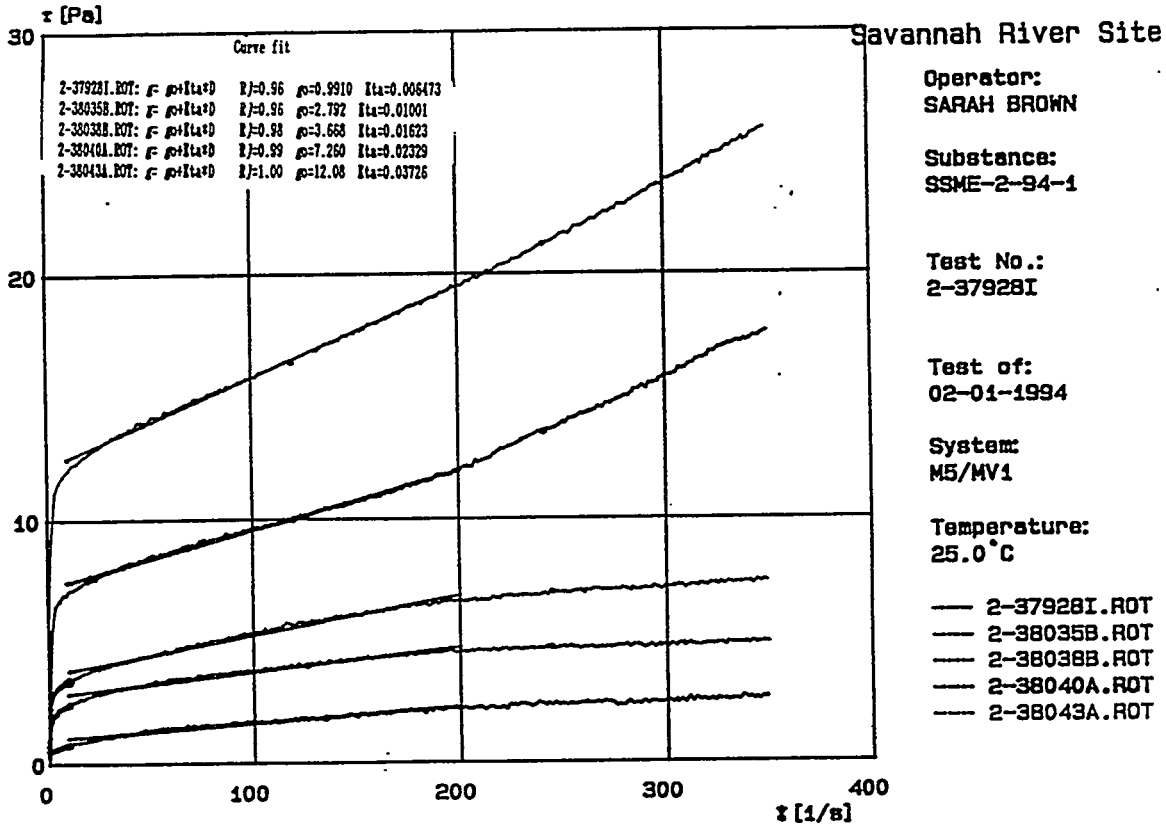

Figure 1: Concentric cylinder viscometer data, shear stress vs strain rate, for simulated melter feed slurries (Marek, 1994).

The non-linear behavior in the rheograms cannot be modelled by a Bingham plastic model in which the stress is assumed to be a linear function of the strain rate once the yield stress is exceeded. Equation 1 is the functional form of a Bingham plastic. This is a two parameter model. In order to model the non-linear behavior, a more complicated model with more degrees of freedom is required. A yield/power law model is a simple three parameter model with which the non-linear behavior can be modelled. Equation 2 is the functional form of a yield/power law model.

$$\tau_{rz} = \tau_o + \eta_o \dot{\gamma} \qquad (1)$$

$$\tau_{rz} = \tau_o + \eta_o (\dot{\gamma})^n \qquad (2)$$

Figure 2 is a plot of the stress versus the strain rate for a yield/power law fluid. Also shown for comparison is the behavior of a Newtonian fluid. The non-Newtonian fluid is viscoplastic in that it exhibits a yield stress, τ_o. The value of the exponent of the strain rate determines whether the fluid is pseudoplastic or dilatant. If $n>1$, the fluid is dilatant, and if $n<1$, the fluid is pseudoplastic. If $n=1$, the fluid is a Bingham plastic.

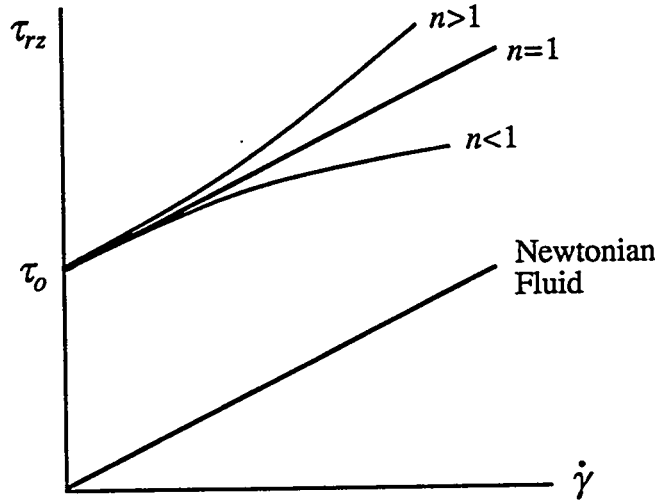

Figure 2: Shear stress versus strain rate for a yield/power law fluid.

Rheological models are necessary for predicting flow versus pressure drop behavior of non-Newtonian fluids. The flow rate versus pressure drop relationships for fully-developed laminar pipe flow for both a yield/power law fluid and a Bingham plastic are derived in Appendix A. Equation 3 is the Buckingham-Reiner equation (Bird, Stewart, & Lightfoot, 1960) for flow rate as a function of pressure drop for a Bingham plastic, and equation 4 is the analogous equation for a yield/power law fluid.

$$Q=\frac{\pi\Delta PR^4}{8L\eta_o}\left[1-\frac{8}{3}\frac{L\tau_o}{\Delta PR}+\frac{16}{3}\left(\frac{L\tau_o}{\Delta PR}\right)^4\right] \tag{3}$$

$$Q=\frac{4\pi Ln}{(n+1)\Delta P\eta_o^{1/n}}\left\{\frac{R^2}{2}\left(\frac{\Delta PR}{2L}-\tau_o\right)^{\frac{n+1}{n}}-\frac{4nL^2}{\Delta P^2}\left[\frac{\left(\frac{\Delta PR}{2L}-\tau_o\right)^{\frac{3n+1}{n}}}{3n+1}+\frac{\tau_o\left(\frac{\Delta PR}{2L}-\tau_o\right)^{\frac{2n+1}{n}}}{2n+1}\right]\right\} \tag{4}$$

Equations 3 and 4 apply only to laminar flow. Fortunately the major differences between Newtonian and non-Newtonian flow occur in the laminar flow regime. Figure 3 is a plot of the Fanning friction factor for pipe flow of a Bingham plastic versus the Reynolds number for several values of the Hedstrom number (Shadday, 1994). Also shown is the laminar relation for a Newtonian fluid, 16/Re. The laminar friction factors for Bingham plastics are significantly larger than those for Newtonian fluids. The start of transition to

turbulent flow for a Bingham plastic occurs at a Reynolds number larger than 2100, the transition Reynolds number for a Newtonian fluid. The actual transition Reynolds number is a function of the fluid properties and the pipe diameter. The turbulent friction factors for fluids with various Hedstrom numbers fall on essentially the same line. These friction factors are very close to the values for turbulent flow of a Newtonian fluid through a smooth pipe. Only laminar flow is considered in this document.

$$\mathrm{Re}_B = \frac{\rho v D}{\eta_o} \qquad He = \frac{\rho \tau_o D^2}{\eta_o^2} \tag{5}$$

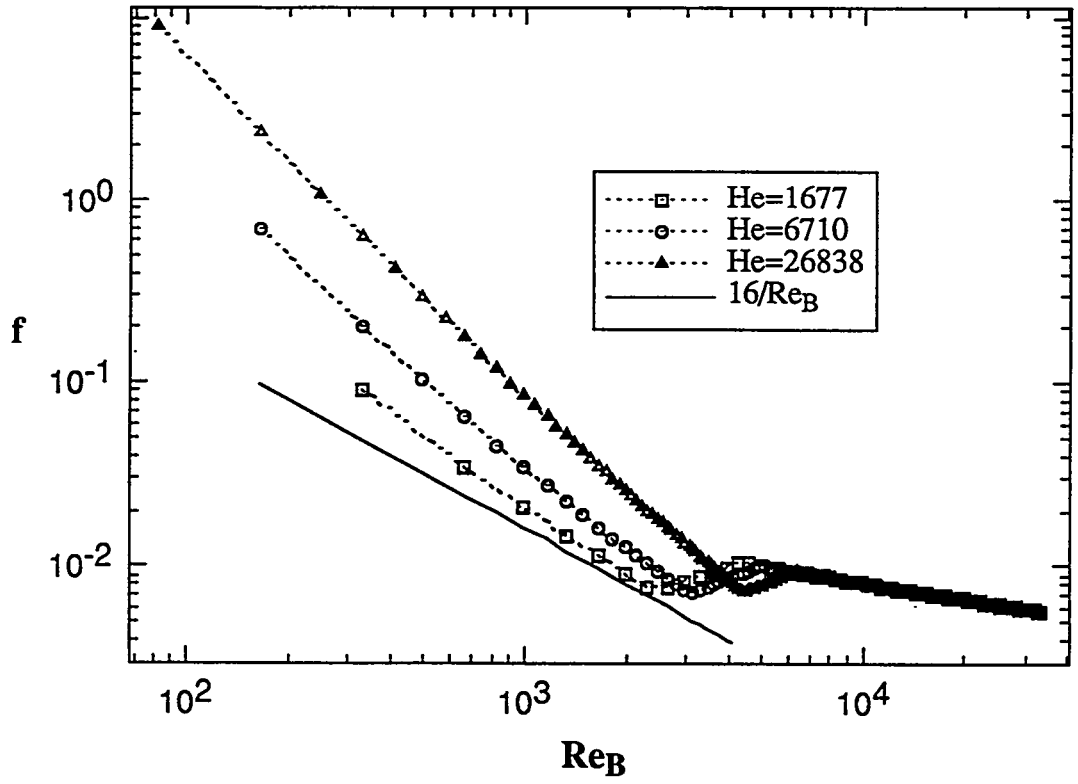

Figure 3: Fanning friction factors for a Bingham plastic.

The transition from laminar to turbulent flow of a Bingham plastic is defined in terms of the Reynolds and Hedstrom numbers. These non-dimensional parameters are defined in equation 5. The transition for a yield/power law fluid is similarly defined. Dimensional analysis of pipe flow of a yield/power law fluid shows that the non-dimensional pressure drop is a function of the length to diameter ratio, the Reynolds number, and the Hedstrom number, equation 6. This equation is derived in Appendix B by application of Buckingham's pi theorem (Gerhart & Gross, 1985). The appropriate definitions for the Reynolds and Hedstrom numbers for a yield/power law fluid are shown in equation 7.

$$\frac{\Delta P}{\rho V^2} = F\left(\frac{L}{D}, \frac{\rho V^{2-n} D^n}{\eta_o}, \frac{\rho \tau_o D^{2n} V^{2(1-n)}}{\eta_o^2}\right) \tag{6}$$

$$\mathrm{Re} = \frac{\rho v^{2-n} D^n}{\eta_o} \qquad He = \frac{\rho \tau_o D^{2n} v^{2(1-n)}}{\eta_o^2} \tag{7}$$

In Appendix C, the appropriate relations for predicting the onset of transition to turbulence of a yield/power law fluid are derived. First equation 8 is used to solve for α_c. This parameter is then substituted into equation 9, which is solved for the critical or transition Reynolds number.

$$\frac{\alpha_c}{(1-\alpha_c)^{\frac{n+2}{2-n}}} = \frac{\rho^{\frac{n}{2-n}} \tau_o R^{\frac{2n}{2-n}}}{\eta_o^{\frac{2}{2-n}}} \left[\frac{n}{808(n+2)^{\frac{n+2}{n+1}}} \right]^{\frac{n}{2-n}} \tag{8}$$

$$\mathrm{Re}_c = \frac{3232 n^{1-n} (n+2)^{\frac{n+2}{n+1}}}{(n+1)^{2-n} (1-\alpha_c)^{\frac{n+2}{n}}} \left[\frac{1}{2}(1-\alpha_c)^{\frac{n+1}{n}} - \frac{n\alpha_c (1-\alpha_c)^{\frac{2n+1}{n}}}{2n+1} - \frac{n(1-\alpha_c)^{\frac{3n+1}{n}}}{3n+1} \right]^{2-n} \tag{9}$$

The analogous relations for a Bingham plastic are equations 10 and 11, (Govier and Aziz, 1972).

$$\frac{\alpha_c}{(1-\alpha_c)^3} = \frac{He}{16800} \tag{10}$$

$$\mathrm{Re}_c = \frac{He}{8\alpha_c} \left(1 - \frac{4}{3}\alpha_c + \frac{1}{3}\alpha_c^4 \right) \tag{11}$$

Bingham plastic and yield/power law models are completely empirical, so you cannot safely extrapolate outside of the range of the data base. The system modelling requirements should therefore determine need for rheological data. The data shown in figure 1 is sufficient for modelling pipe flows in which the absolute value of the wall velocity gradient (strain rate) is less than 350 1/s. In the next section, this will be shown to be quite limiting.

Analysis and Results

Predicted pipe flows for Bingham plastic and yield/power law models of the fluids with the top three rheograms in figure 1 are compared. The three rheograms are for slurries with 54.17%, 49.36%, and 47.34% total weight solids respectively from the top. Ten points were picked off each of the rheograms and a yield/power law model, equation 2, was fit to the data. Figures 4 through 6 show the ten data points, the yield/power law model, and the Bingham plastic model that Jim Marek determined, for the three rheograms. The Bingham plastic model was determined from the data up to a strain rate of 200 1/s. The legends in figures 4 through 6 show the model parameters.

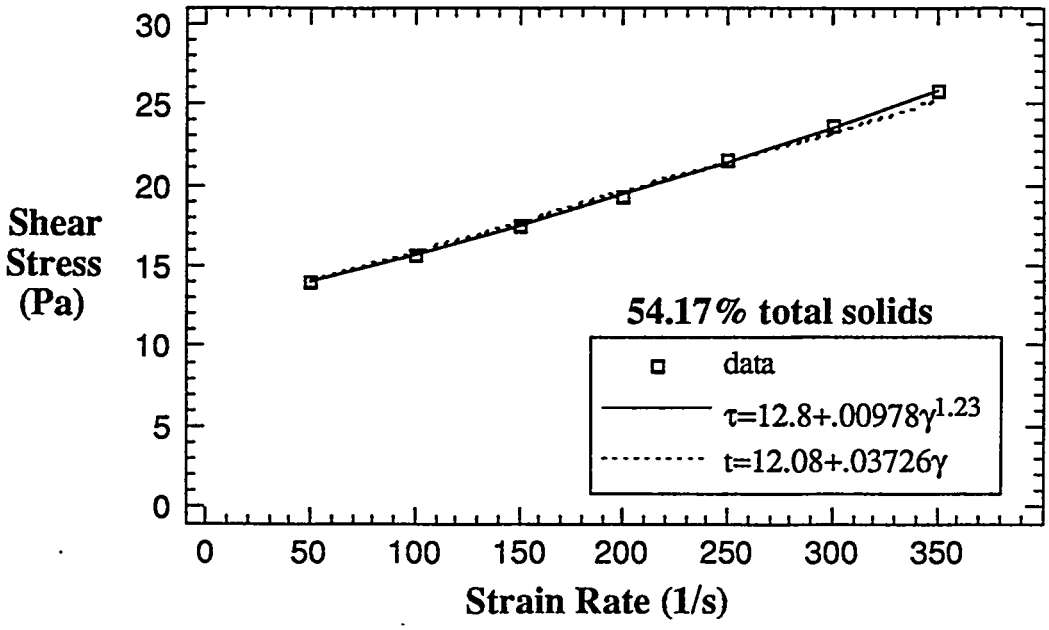

Figure 4: Bingham plastic and yield/power law models of the 54.17% total weight solids slurry.

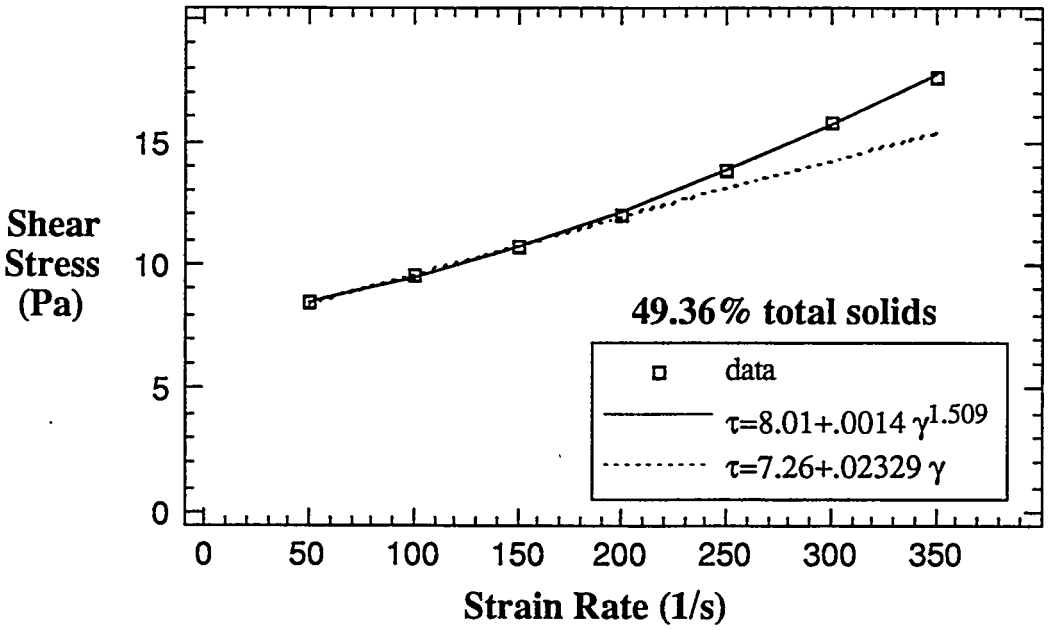

Figure 5: Bingham plastic and yield/power law models of the 49.36% total weight solids slurry.

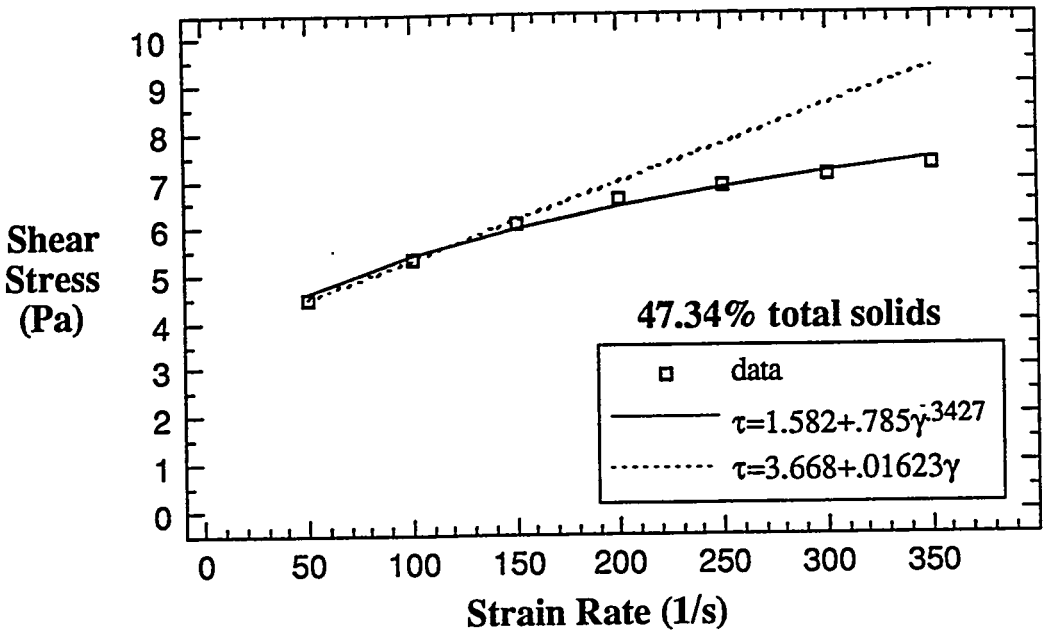

Figure 6: Bingham plastic and yield/power law models of the 47.34% total weight solids slurry.

Figures 7 through 9 show the predicted flow rates of the three slurries through the 3/8" melter feed line, as a function of the frictional pressure drop. These flow rates are calculated with equation 3 for the Bingham plastic fluids and equation 4 for the yield/power law fluids. The assumed length of the pipe is 16.217 m. This is the equivalent length of the 3/8" line in melter feed system #2, (Shadday, 1994). The diameter of the line is .01074 m. The plots span the range of strain rates from 50 to 350 1/s. The wall strain rates are calculated from the Bingham plastic and yield/power law fluid governing equations, equations 1 and 2 respectively. The wall stress values that are used in these equations are calculated from the axial pressure drops, equation 12.

$$\tau_\omega = \frac{\Delta P}{2L} R \qquad (12)$$

There is good agreement between the Bingham plastic and the yield/power law fluid flow rates for the 54.17% total weight solids slurry. The two rheological models for this slurry are also in good agreement over the entire range of strain rates. The other two slurries show significant differences between the predicted flow rates of the two rheological models at higher strain rates. The Bingham plastic model predicts higher flow rates than the yield/power law model, at the upper end of the range of pressure drops, for the 49.36% total weight solids slurry, and the opposite behavior is predicted for the 47.34 % total weight solids slurry. In both cases the yield/power law models should be better since they are in better agreement with the rheological data. For the dilatant fluid, the Bingham plastic model over predicts the flow rate, and for the pseudo plastic fluid, the Bingham plastic model under predicts the flow rate. The danger of extrapolating beyond a strain rate of 350 1/s is evident in figures 8 and 9. The differences between the predicted flow rates for the two rheological models increase rapidly with increasing flow rate.

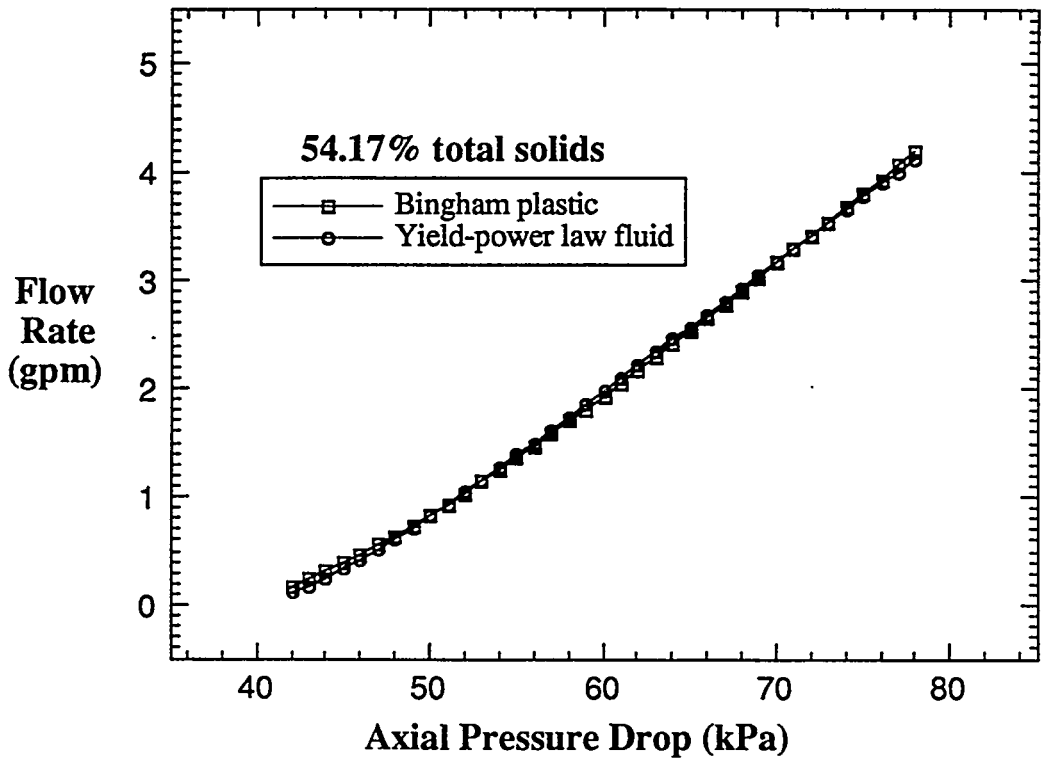

Figure 7: Flow rate through the melter feed line as a function of the frictional pressure drop.

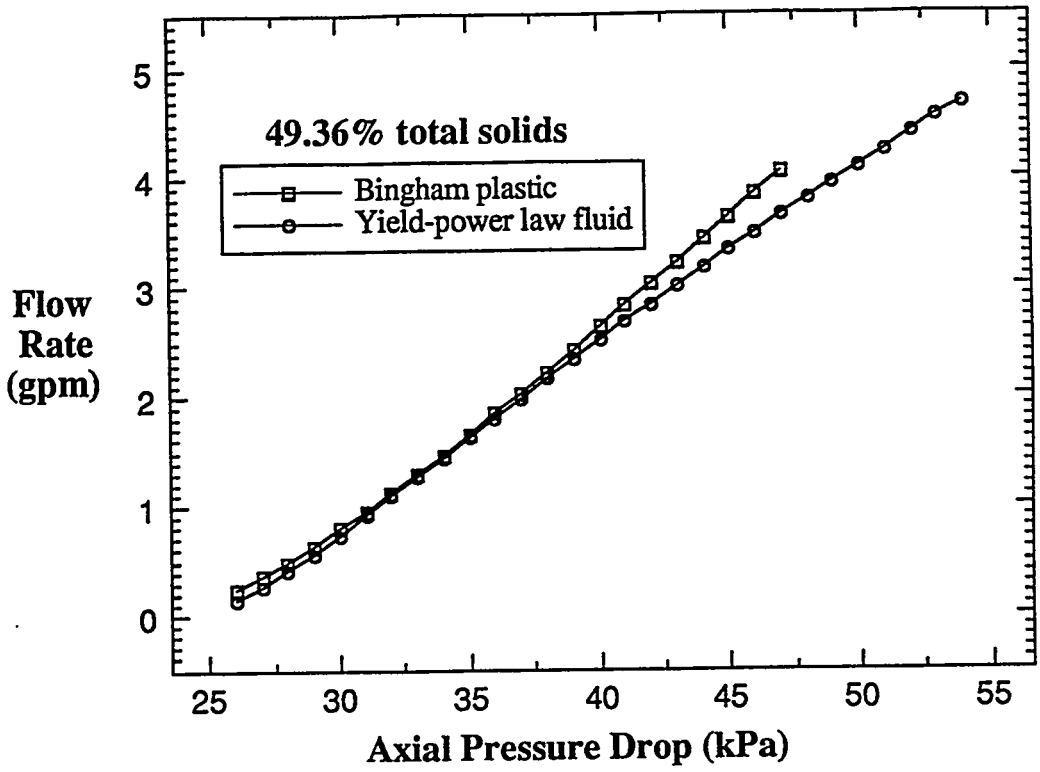

Figure 8: Flow rate through the melter feed line as a function of the frictional pressure drop.

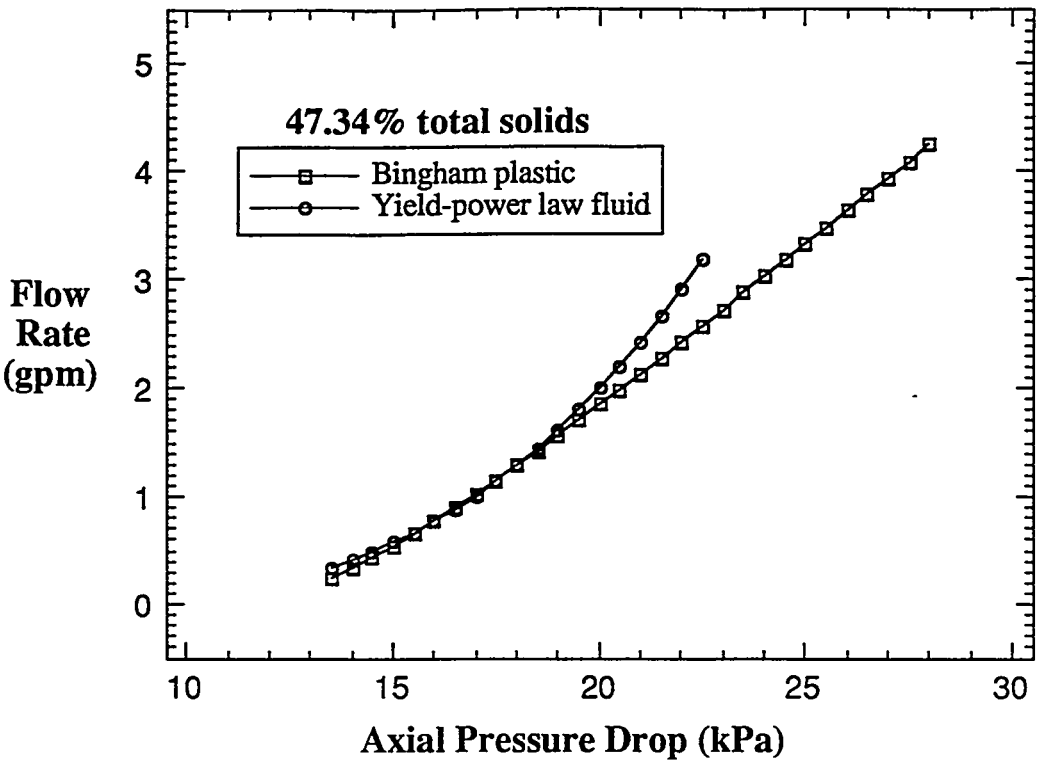

Figure 9: Flow rate through the melter feed line as a function of the frictional pressure drop.

The Reynolds numbers of the predicted flows, as functions of the wall strain rate, are shown in figure 10. The Bingham plastic Reynolds number is defined by equation 5, and the yield/power law fluid Reynolds number is defined by equation 7. Figure 11 shows the Reynolds numbers as functions of the flow rate. The yield/power law Reynolds number can differ significantly from the Bingham plastic Reynolds number. The yield/power law Reynolds number for the 47.34% total weight solids slurry, a pseudoplastic fluid, is much lower than the Bingham plastic Reynolds number, and the yield/power law Reynolds number for the 49.36% total weight solids slurry, a dilatant fluid, is much higher than the Bingham plastic Reynolds number. This suggests that the Reynolds numbers of the various rheology models cannot be compared, but the Reynolds number has significance only in the context of a specific rheological model.

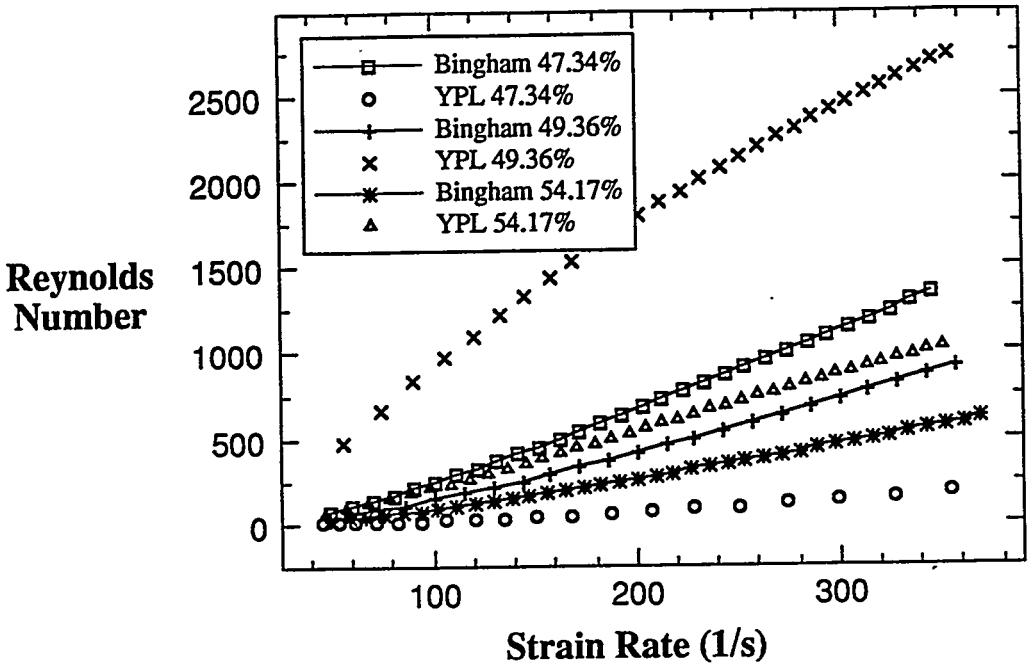

Figure 10: Reynolds number versus strain rate for flow through a 3/8" pipe.

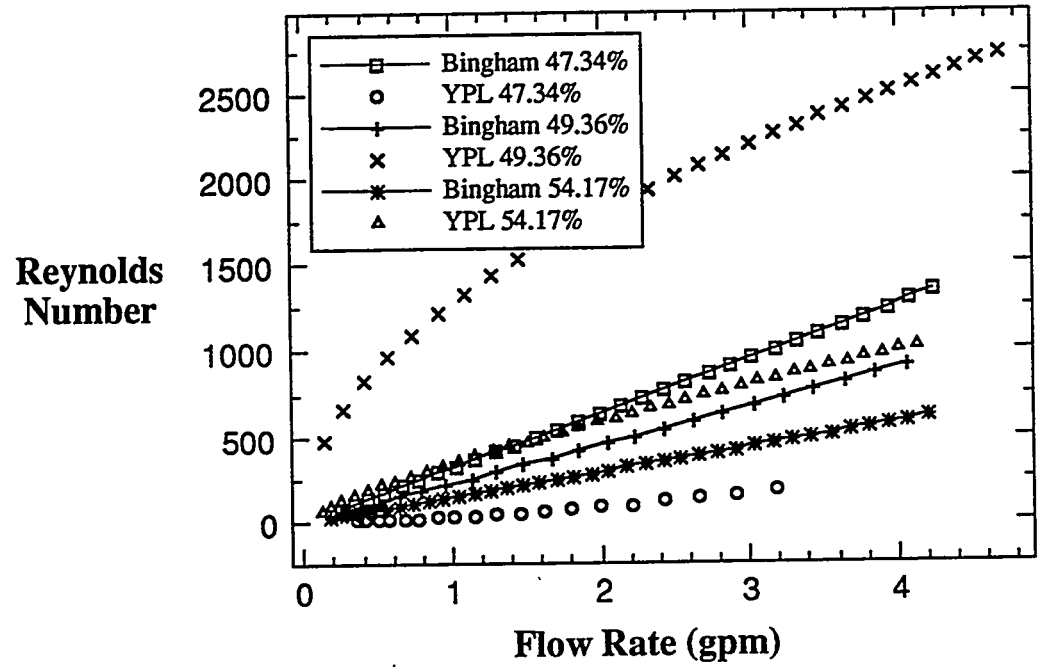

Figure 11: Reynolds number versus flow rate for flow through a 3/8" pipe.

Whether a flow is laminar or turbulent is a function of the Reynolds number. The transition Reynolds number for flow of a yield/power law fluid is calculated with equations 8 and 9, and for a Bingham plastic with equations 10 and 11. The predicted transition Reynolds numbers for the three slurries are shown in table 1. The transition

Reynolds numbers for the three Bingham plastic models are grouped closely together, while those of the yield/power law models are spread over a wide range. In all cases the predicted transition Reynolds numbers are considerably larger than the Reynolds numbers with a wall strain rate of 350 1/s. The rheological data in figure 1 falls well short of covering the laminar flow range. For the melter feed line, this data is adequate because the expected flow rates are between 0.4 and 1.0 gpm, and the data covers the wall strain rate range that corresponds to flow rates of approximately 4.0 gpm.

% Total Wt. Solids	Rheological Model	Transition Re	Re at Wall Strain Rate = 350 1/s
54.17%	yield/power law	3138.6	1028.2
	Bingham plastic	2366.1	569.8
49.36%	yield/power law	4692.5	2719.4
	Bingham plastic	2475.4	890.1
47.34%	yield/power law	795.7	171.9
	Bingham plastic	2483.2	1368.4

Table 1: Calculated laminar to turbulent flow transition Reynolds numbers for the rheological models of the three slurries shown in figures 4 through 6.

The sample line of the Slurry Mix Evaporator (SME) sampling system is a 1/2" schedule 40 pipe that is approximately 42 m in length. The range of expected flow rates is between 4 and 10 gpm, and therefore the expected wall strain rates will exceed 350 1/s. The rheological data shown in figure 1 is inadequate to form a basis for modelling this flow. In order to show the potential errors introduced by using a Bingham plastic model based on low strain rate data to describe the flow behavior of a fluid that is more appropriately modelled as a yield/power law fluid, two examples are considered, one with a dilatant fluid and the other with a pseudoplastic fluid. Figure 12 shows the assumed rheological behavior of the two example fluids over the entire laminar flow range. The rheograms cover the strain rate range from 50 to 2400 1/s.

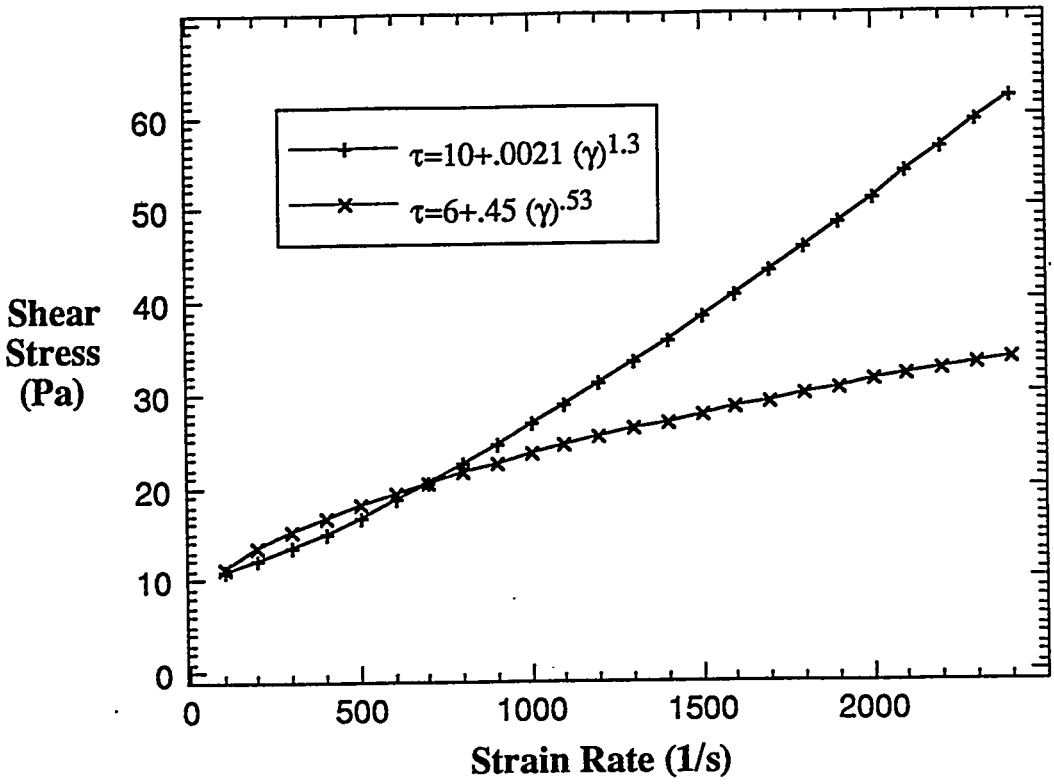

Figure 12: Rheograms of two assumed yield/power law fluids.

Figure 13 shows the shear stress versus strain rate behavior of the assumed dilatant yield/power law fluid in figure 12. Also shown are two Bingham plastic models of the same fluid, one is based on the entire range of strain rates, and the other is based on the strain rates up to 300 1/s. The second Bingham plastic model is the one that would be derived from concentric cylinder viscometer data.

Flow rates in the SME sample line of fluids with the three constituitive relations shown in figure 13 are calculated as functions of the frictional pressure drop. The diameter of the pipe is .007874 m, and the length is 52.4 m. The length includes equivalent lengths for elbows. The predicted flow rates as functions of the pressure drop are shown in figure 14. The plots of flow rates go up to the point that transition from laminar to turbulent flow is predicted to occur. The predicted transition Reynolds numbers for the three fluid rheological models are shown in table 2. For all three fluid models, transition occurs at a flow rate of approximately 8.0 gpm, for flow in the SME sample line.

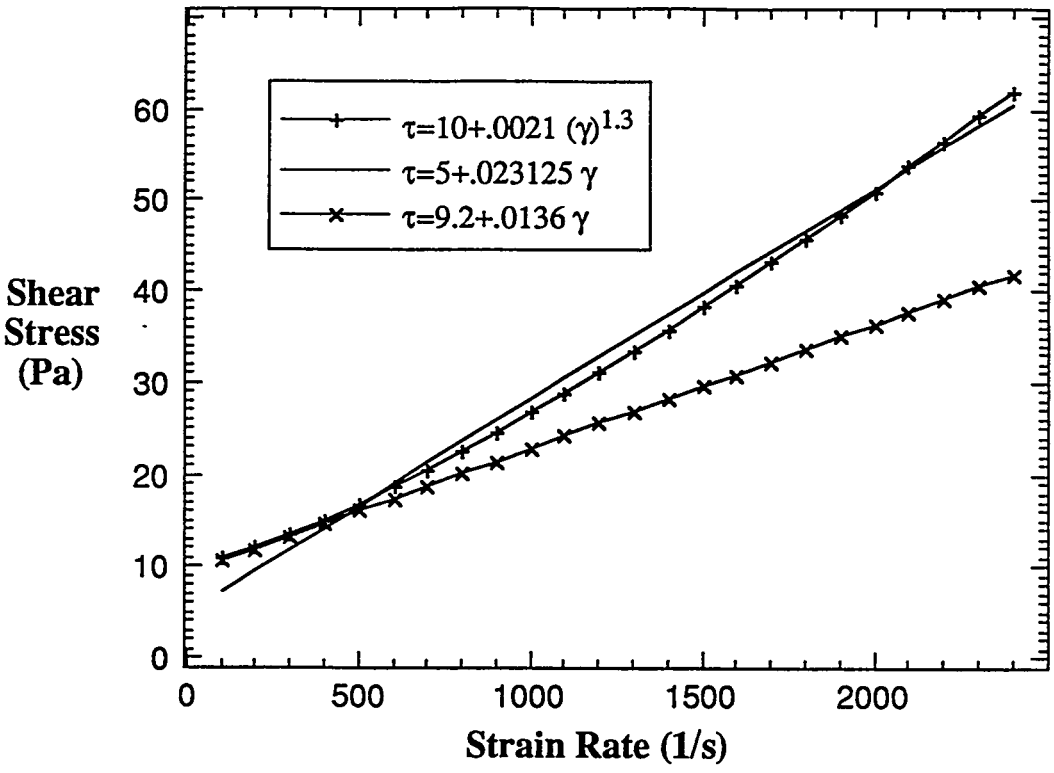

Figure 13: The assumed dilatant yield/power fluid and two Bingham plastic models of the fluid, one based on the entire strain rate range, and the other based on the strain rate up to 300 1/s.

Rheological Model	**Transition Reynolds Number**
$\tau = 10+.0021\dot{\gamma}^{1.3}$	Re_c=5923.4
$\tau = 5+.023125\dot{\gamma}$	Re_c=2627.3
$\tau = 9.2+.0136\dot{\gamma}$	Re_c=3863.7

Table 2: Laminar to turbulent flow transition Reynolds numbers for the slurries in figure 13.

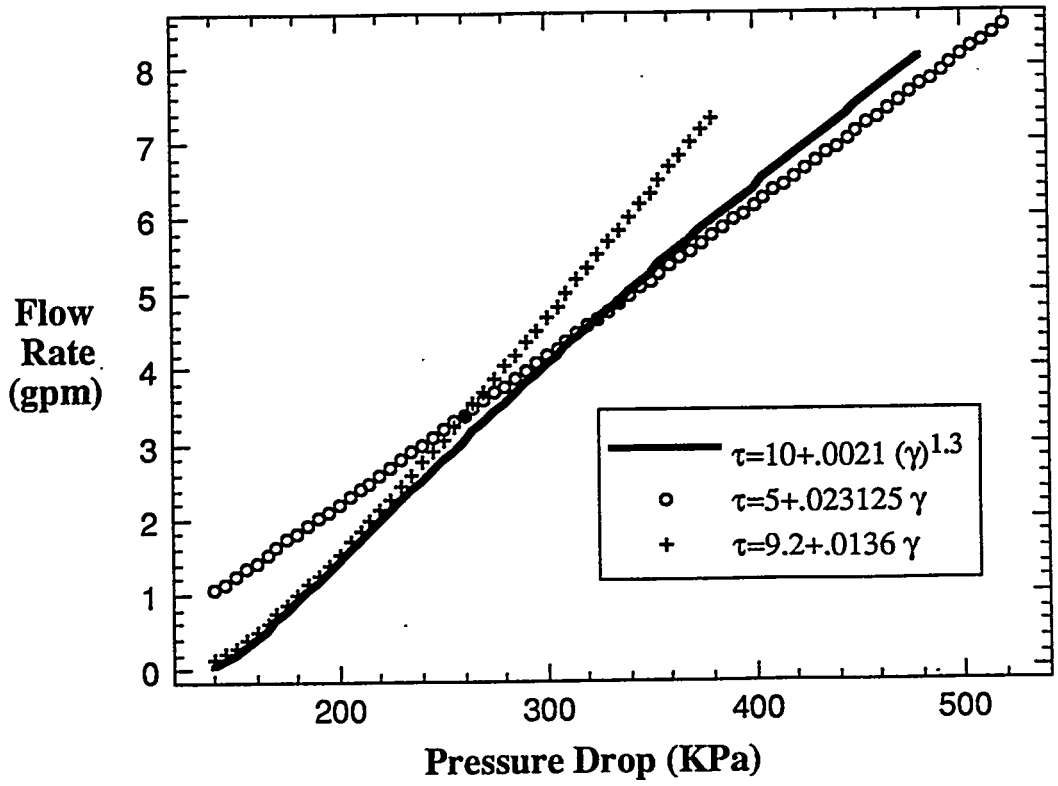

Figure 14: Flow rate through the SME sample line of the assumed dilatant yield/power law fluid as a function of the frictional pressure drop. Also shown are the predicted flow rates of the two Bingham plastic models of the same fluid.

As you would expect, flow rates of the Bingham plastic model based on strain rates below 300 1/s agree well with the lower flow rates of the yield/power law fluid, and the Bingham plastic model based on the entire strain rate range agrees better with the yield/power law model at higher flow rates. For this assumed fluid, a single Bingham plastic model is inadequate to model flows in both the melter feed lines and the sample lines. The Bingham plastic model based on strain rates below 300 1/s is clearly better for the melter feed line, where flow rates are less than one gpm, and the other Bingham plastic model is better for the sample line, in which the flow rates are between 4 and 8 gpm. A constituitive relation that is in good agreement with the rheological data over the entire laminar range is the best alternative, and a yield/power law model, with the extra parameter, can fit real data better than a Bingham plastic model.

Figure 15 shows the Reynolds numbers as functions of the wall strain rate for the three fluid models. While the laminar/turbulent transition Reynolds numbers differ significantly for the three fluid models, transition is predicted to occur at a wall strain rate between 1400 and 1500 1/s. To reasonably model flows in the sample line, rheological data must be collected with strain rates up to transition.

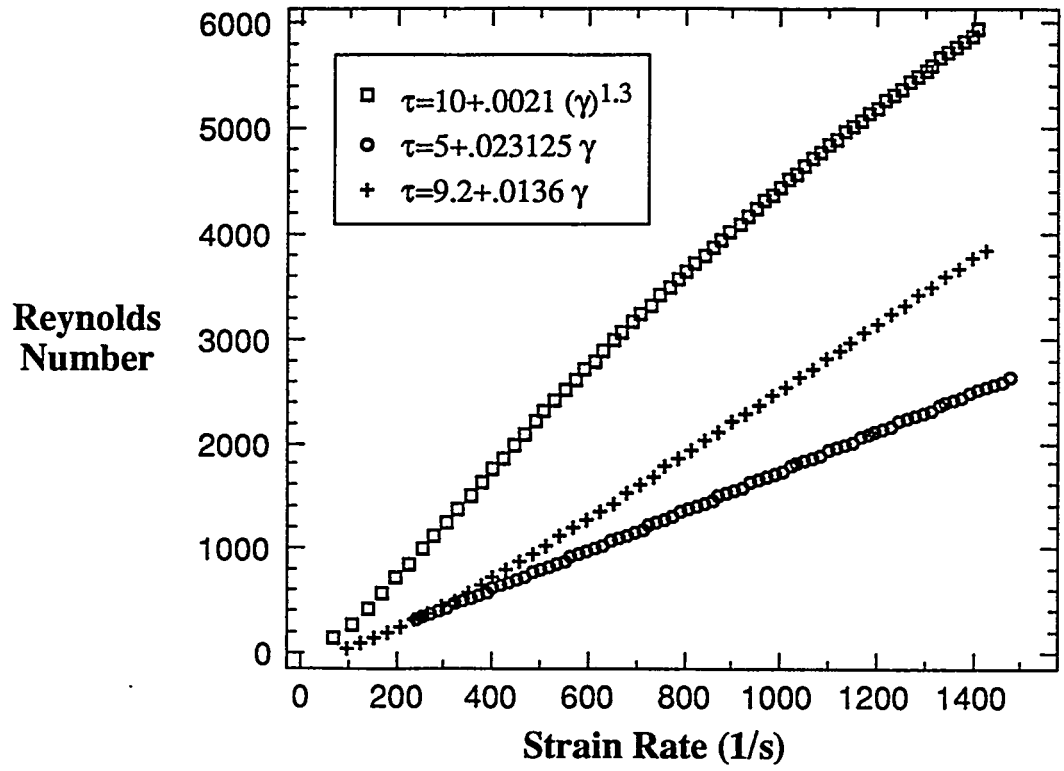

Figure 15: Reynolds numbers in the SME sample line as functions of the wall strain rates.

Figure 16 shows the percent error in the predicted flow rates of the two Bingham plastic models of the assumed fluid, relative to the predicted flow rate of the yield/power law model. At very low flow rates, the relative errors of both Bingham plastic models are large, but the absolute flow rates are small so the absolute errors are small. The relative error of the model based on strain rate data below 300 1/s increases linearly for flow rates above 2.0 gpm, and the relative error is 25% at the predicted transition to turbulence. This plot clearly shows the danger of extrapolating the constituitive relations beyond the range of the data on which it is based.

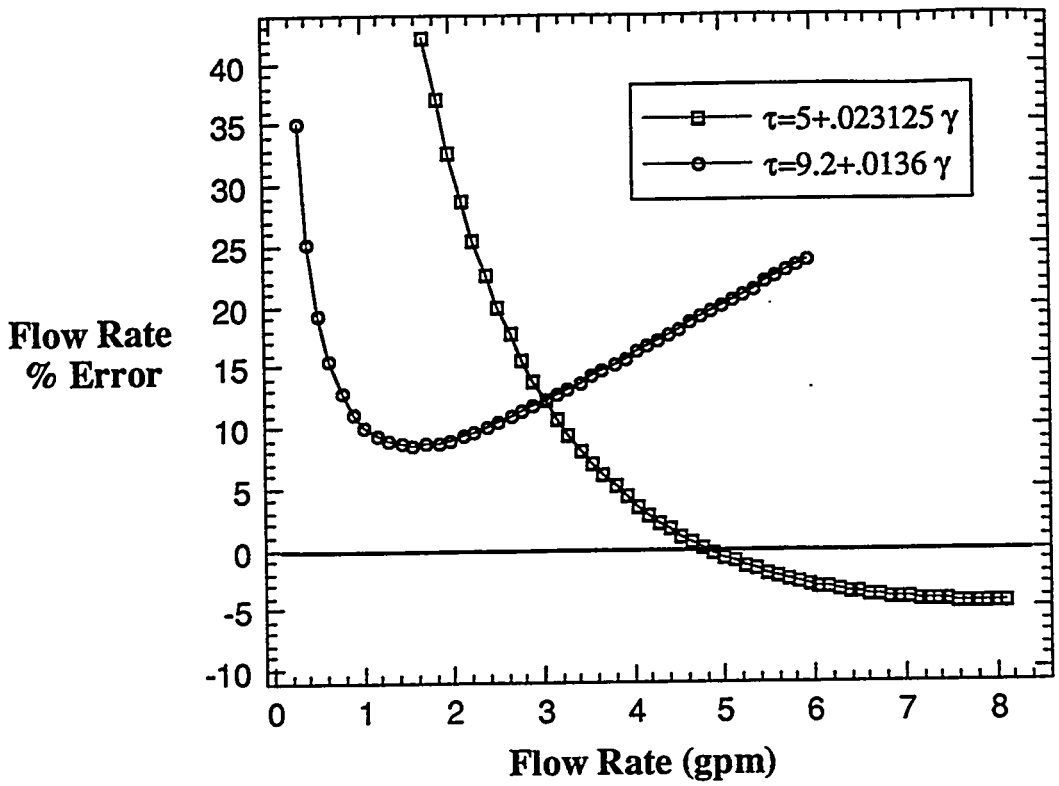

Figure 16: Percent error in the predicted flow rates in the SME sample line for the two Bingham plastic models, relative to the yield/power law model.

The results of similar calculations with the pseudoplastic fluid shown in figure 12 are presented in figures 17 through 20. The results are similar to those for the dilatant fluid, and the same conclusions apply. Transition to turbulence occurs at a slightly higher flow rate, between 8.0 and 9.0 gpm, than with the dilitant fluid, and the wall strain rate at transition is also higher, between 1500 and 1800 1/s. Figures 17 through 20 correspond respectively with figures 13 through 16, and they are presented without further discussion.

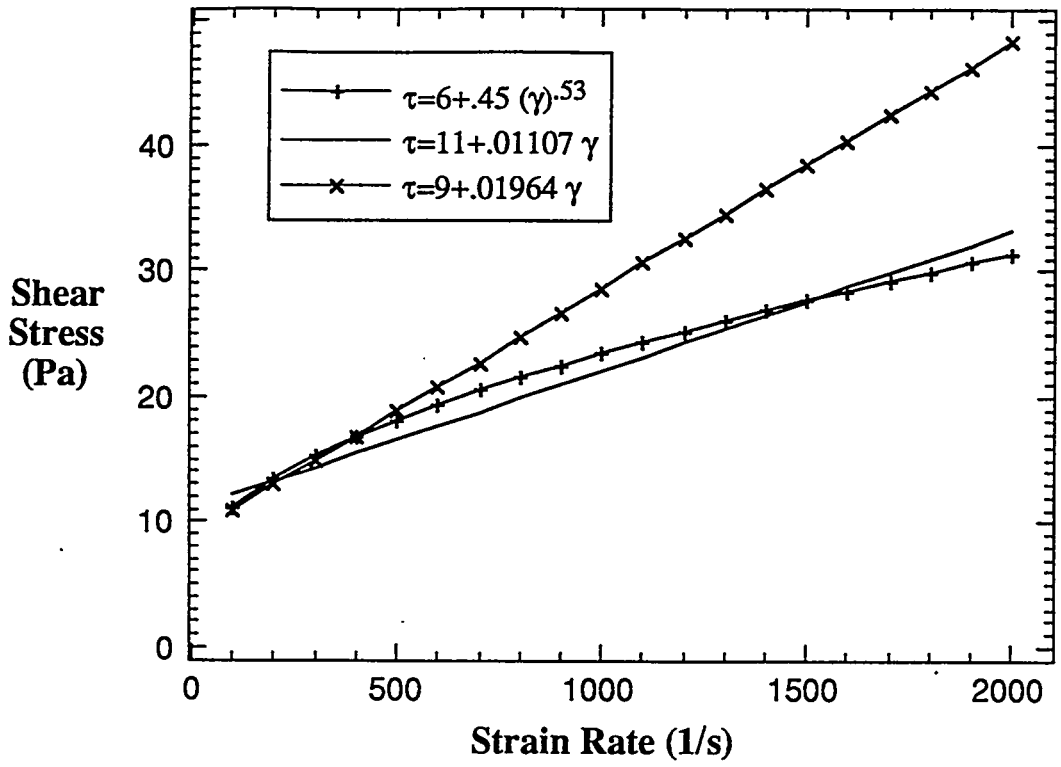

Figure 17: The assumed pseudoplastic yield/power fluid and two Bingham plastic models of the fluid, one based on the entire strain rate range, and the other based on the strain rate up to 300 1/s.

Rheological Model	**Transition Reynolds Number**
$\tau = 6+.45\dot{\gamma}^{.53}$	Re_c=1308.4
$\tau = 11+.01107\dot{\gamma}$	Re_c=4622.6
$\tau = 9+.01964\dot{\gamma}$	Re_c=3160.0

Table 3: Laminar to turbulent flow transition Reynolds numbers for the slurries in figure 17.

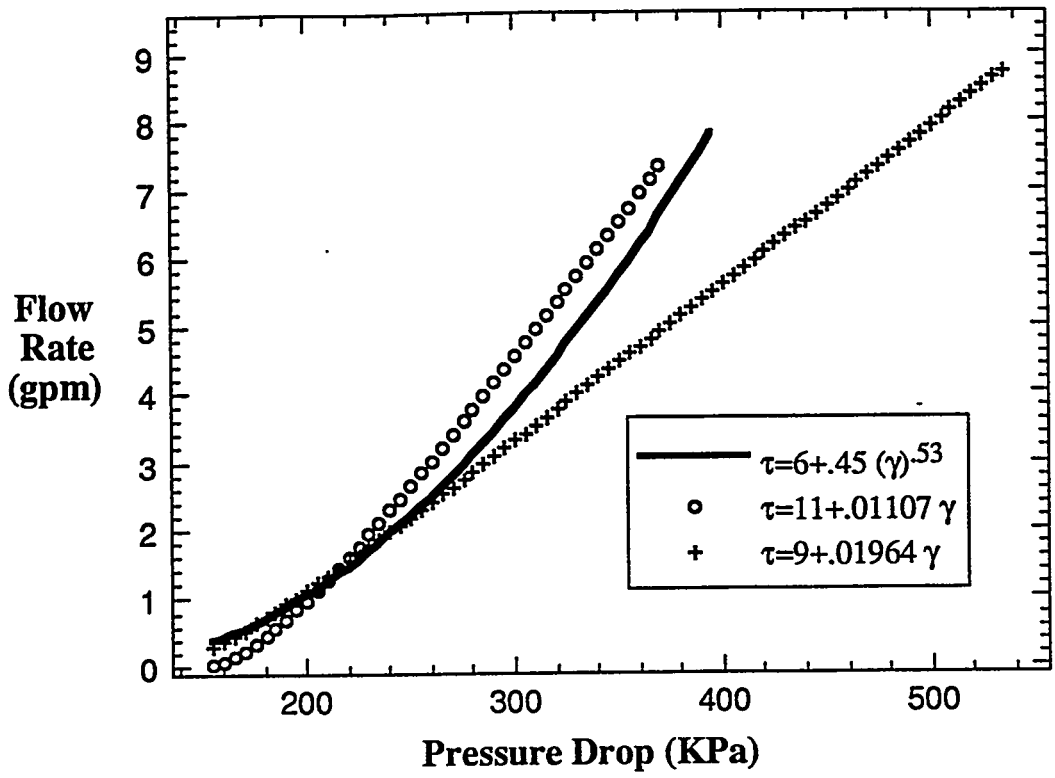

Figure 18: Flow rate through the SME sample line of the assumed pseudoplastic fluid as a function of the frictional pressure drop. Also shown are the predicted flow rates of the two Bingham plastic models of the same fluid.

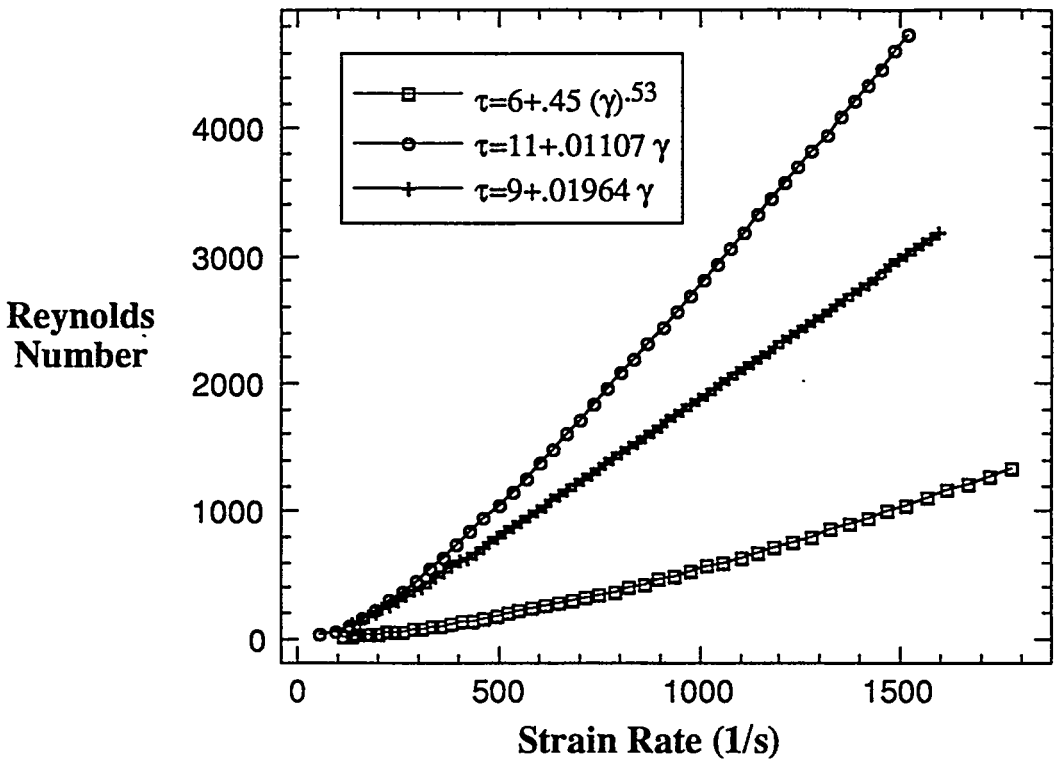

Figure 19: Reynolds numbers in the SME sample line as functions of the wall strain rates.

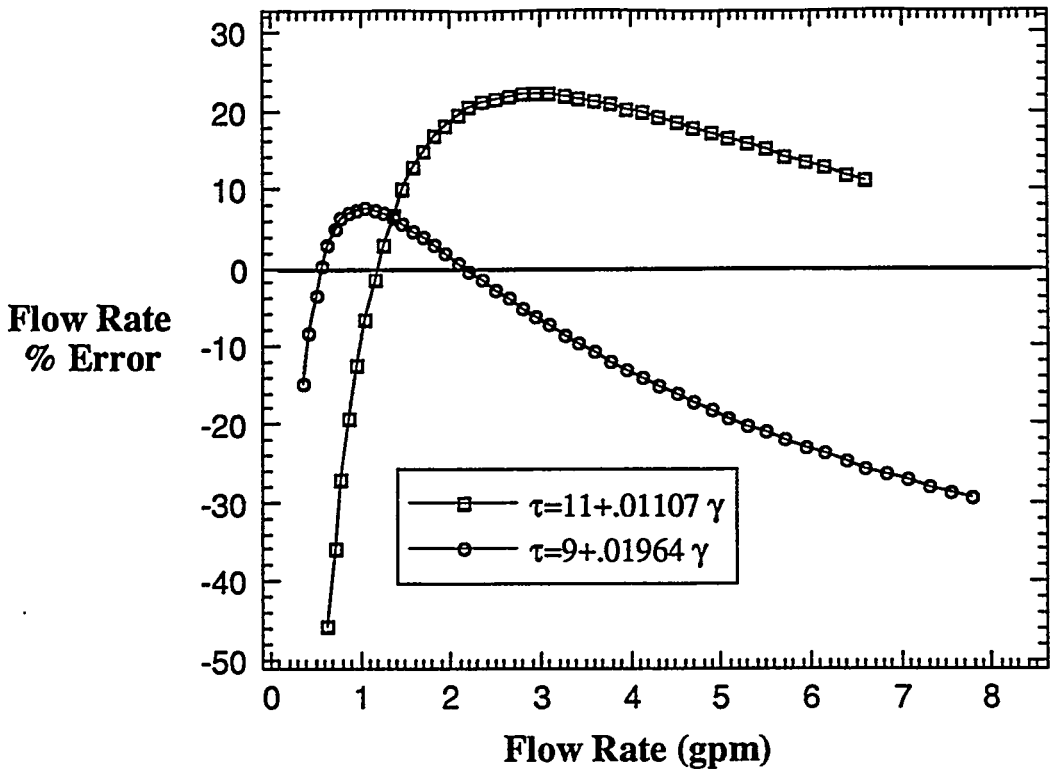

Figure 20: Percent errors in the predicted flow rates in the SME sample line for the two Bingham plastic models, relative to the yield/power law model.

It is difficult to obtain high strain rate data with a concentric cylinder viscometer, because of centrifugal effects and wall slip. Good low strain rate data, that allow determination of the yield stress, can be obtained with this type of viscometer. The interpretation of data collected with a concentric cylinder visometer is also straightforward. A capillary viscometer is a device in which the axial pressure drop of fully-developed flow through a straight tube is measured. The laminar flow range up to transition can easily be covered with this type of viscometer, though it is not ideal for measuring the behavior of fluids at very low flow rates, or wall strain rates. The two types of viscometer are therefore complementary, and they can be used to cover the rheometry of slurries from the yield stress up to the transition to turbulence.

A capillary viscometry is simple and inexpensive. All one needs to do is measure the axial pressure drop in a straight pipe in which the flow is fully-developed. The data to be collected is the pressure drop and the flow rate. This data can be converted to shear stress versus strain rate data with the Rabinowitsch equation, equation 13, (Bird, Stewart, & Lightfoot, 1960).

$$-\left(\frac{dv_z}{dr}\right)_{r=R} = \frac{1}{\pi R^3 \tau_R^2}\frac{d}{d\tau_R}\left(\tau_R^3 Q\right) \qquad (13)$$

The left side of equation 13 is the absolute value of the wall strain rate. By substituting equation 12 for the wall shear stress and expanding the differential term on the right side of equation 13, the wall strain rate can be expressed as a function of the flow rate and the pressure drop, in a form convenient for calculatng the wall strain rate, equation 14.

$$\dot{\gamma} = \frac{Q}{\pi R^2}\left(\frac{d(\ln Q)}{d(\ln \Delta P)} + 3\right) \qquad (14)$$

The strain rate can be obtained directly from a plot of the natural log of the flow rate versus the natural log of the pressure drop. If pressure drop versus flow rate data is obtained up to the point of transition to turbulent flow, and low strain rate data is obtained with a concentric cylinder viscometer, a plot of shear stress versus strain rate for the entire laminar range can be easily made.

Conclusions

Flow rates over the entire laminar flow range are encountered in the SME sample system, and the data bases for rheological models of the slurries of interest must also cover the entire laminar range, if reasonable hydraulic models of the sample system are expected. The results of the analysis of flow through the 1/2" schedule 40 sample line of the two hypothetical slurries, with rheograms shown in figure 12, clearly show the danger of extrapolating rheological models based on data that cover a small part of the laminar flow range. The analysis shows the danger of extrapolating Bingham plastic models, based on strain rate data up to 350 1/s, up to the point of transition to turbulent flow, which is expected to occur at a wall strain rate of approximately 1500 1/s. The danger of extrapolation is equally applicable to more complicated models such as yield/power law fluids. The data base must cover the range of laminar wall strain rates expected to be encountered, because the rheological models developed from the data are completely empirical.

With rheological data that spans the entire laminar range, good rheological models can be developed. The yield/power law model, with one more degree of freedom than the Bingham plastic model, is better able to fit data over a wide range of strain rates. Equations for predicting the flow rate versus pressure drop relationship and the point of transition to turbulent flow have been derived for a yield/power law fluid, so all of the calculative tools for analyzing flows in hydraulic networks are available. Whether a single model can adequately fit the data over the entire laminar range or several models have to be tacked together in a piecemeal fashion, can be determined only after the rheology data is obtained and plotted.

References

Bird, R. B., Armstrong, R. C., Hassager, O., 1987, Dynamics of Polymeric Liquids, Volume 1 Fluid Mechanics, John Wiley & Sons.

Bird, R. B., Stewart, W. E., Lightfoot, E. N., 1960, Transport Phenomena, John Wiley & Sons.

Gerhart, P. M., Gross, R. M., 1985, Fundamentals of Fluid Mechanics, Addiso -Wesley Publishing Company.

Govier, G. W., and Aziz, K., 1972, The Flow of Complex Mixtures in Pipes, Van Nostrand Reinhold Company.

Hanks, R. W., 1963, "The Laminar-Turbulent Transition for Fluids with a Yield Stress", *A. I. Ch. E. Journal*, Volume 9, #3, May 1963.

Marek, J. C., 1994, personnal conversation, the rheogram was obtained from his laboratory notebook.

Shadday, M. A., 1994, "DWPF Melter Feed System; Model Description and Results (U)", WSRC-TR-94-0215, April 1994.

This Page Intentionally Left Blank

Appendix A Pressure Drop/Flow Rate Equations

The relationship between the laminar flow rate and the frictional pressure drop for fully-developed flow of a yield/power law non-Newtonian fluid is developed in this appendix. The Buckingham-Reiner equation for a Bingham plastic (Bird, Stewart, & Lightfoot, 1960) will be shown to be a special case of the yield/power law fluid relation, with an exponent equal to one. As a first step, the relation for the shear distribution in fully-developed pipe flow will be derived.

Consider fully-developed and steady flow of an incompressible fluid through a straight pipe with a circular cross-section. The continuity equation for this flow is equation a1.

$$\frac{1}{r}\frac{\partial}{\partial r}(rv_r)+\frac{1}{r}\frac{\partial v_\theta}{\partial \theta}+\frac{\partial v_z}{\partial z}=0 \qquad \text{(a1)}$$

The flow is assumed to possess azimuthal symmetry, and since it is also fully-developed, the azimuthal and radial velocity components are zero. The continuity equation therefore simplifies to an expression stating that the axial gradient of the axial velocity component is equal to zero:

$$\frac{\partial v_z}{\partial z}=0 \qquad \text{(a2)}$$

The shear distribution is determined by applying the integral form of the momentum equation, equation a3, to the annular control volume shown in figure a1.

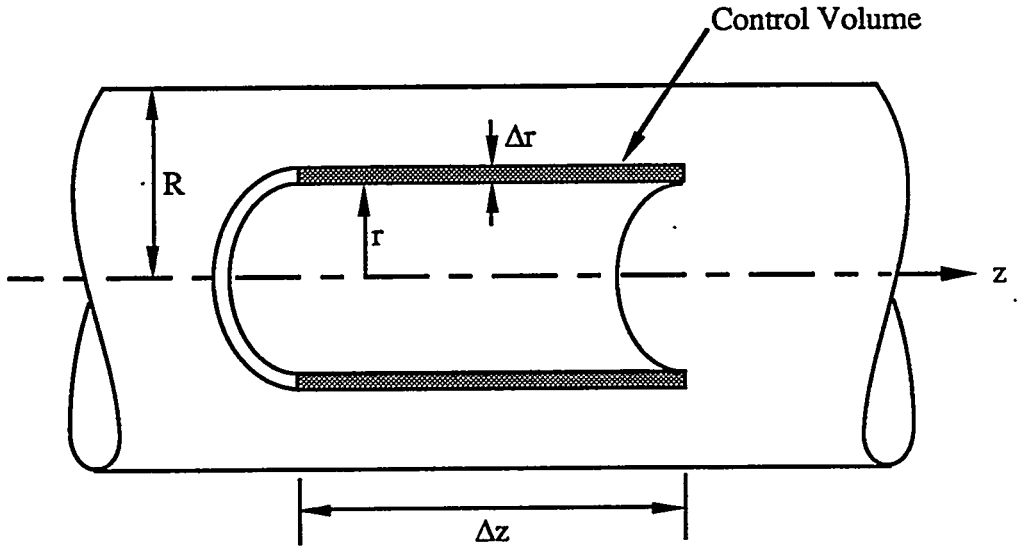

Figure A1: An annular control volume for axisymmetric flow in a pipe.

$$\sum \vec{F}=\frac{\partial}{\partial t}\int_{Vol}\rho\vec{V}d(Vol)+\oint_A \rho\vec{V}\left(\vec{V}\bullet d\vec{A}\right) \qquad \text{(a3)}$$

For steady flow, the first integral on the right side of equation a3 is zero. The second integral term is an expression for the net rate at which momentum is convected into the control volume, and this is equated with the sum of the forces acting on the control volume. Figure A2 shows the surface forces acting on, and the momentum rates entering and leaving the control volume. Expressions for the areas of the surfaces of the control volume are shown in equation a4.

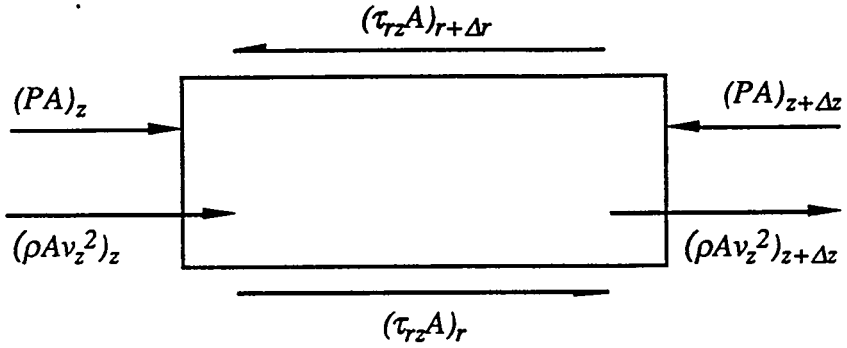

Figure A2: Forces and convective momentum rate applicable to the annular control volume.

$$\begin{aligned} A_r &= 2\pi r\Delta z \\ A_{r+\Delta r} &= 2\pi(r+\Delta r)\Delta z \\ A_z &= A_{z+\Delta z} = \pi\left[2r\Delta r+(\Delta r)^2\right] \end{aligned} \tag{a4}$$

Equation a5 is the expression for the sum of the forces acting on the control volume, and equation a6 is the expression for the net momentum rate convected into the control volume. The convective term is equal to zero since the axial velocity gradient is zero.

$$\begin{aligned} \sum F_z = P_z\pi\left(2r\Delta r+(\Delta r)^2\right) - P_{z+\Delta z}\pi\left(2r\Delta r+(\Delta r)^2\right) + \\ \tau_{rz}\big|_r 2\pi r\Delta z - \tau_{rz}\big|_{r+\Delta r} 2\pi(r+\Delta r)\Delta z \end{aligned} \tag{a5}$$

$$\oint_A \rho\vec{V}\left(\vec{V}\bullet d\vec{A}\right) = \rho\pi\left(2r\Delta r+\Delta r^2\right)\left[(v_z)^2_{z+\Delta z} - (v_z)^2_z\right] = 0 \tag{a6}$$

Equation a7 is the integral form of the momentum equation for the control volume shown in figures A1 and A2. In the limit as the control volume approaches a differential control volume, the two difference terms in equation a7 become differentials, equation a8.

$$\frac{P_z - P_{z+\Delta z}}{\Delta z} + \frac{2}{\Delta r(2r+\Delta r)}\left[(r\tau_{rz})_r - (r\tau_{rz})_{r+\Delta r}\right] = 0 \tag{a7}$$

$$\lim_{\Delta z\to 0}\frac{P_{z+\Delta z}-P_z}{\Delta z} = \frac{dP}{dz} \qquad \lim_{\Delta r\to 0}\frac{(r\tau_{rz})_{r+\Delta r}-(r\tau_{rz})_r}{\Delta r} = \frac{d}{dr}(r\tau_{rz}) \tag{a8}$$

The resultant differential equation for the radial dependence of the shear force, equation a9, is integrated with the boundary condition that the shear force is finite at the centerline.

The resultant differential equation for the radial dependence of the shear force, equation a9, is integrated with the boundary condition that the shear force is finite at the centerline. The solution, equation a10, is the radial shear distribution for fully-developed steady laminar flow of an incompressible fluid through a pipe. This equation is applicable to both flows of Newtonian fluids and fluids that exhibit non-Newtonian viscosity effects, such as a Bingham fluid or a yield/power law fluid.

$$\frac{1}{r}\frac{d}{dr}(r\tau_{rz}) = -\frac{dP}{dz} \tag{a9}$$

$$\tau_{rz} = -\frac{dP}{dz}\frac{r}{2} \tag{a10}$$

Equation a11 is the constitutive equation for a yield/power law fluid.

$$\tau_{rz} = \tau_o + \eta_o\left(-\frac{\partial v_z}{\partial r}\right)^n = \tau_o + \eta_o\dot{\gamma}^n \tag{a11}$$

Figure A3 is a plot of the radial distributions of shear stress and the axial velocity for fully-developed laminar flow through a pipe. The shear stress is zero at the centerline and it increases linearly to a maximum at the wall. The velocity distribution is characterized by two distinct regions: there is a central region of uniform flow, where the shear stress is less than the yield stress, and an annular region with a radially varying velocity profile, where the shear stress is greater than the yield stress. The threshold radius where the shear stress is equal to the yield stress is r_o.

If equation a10 is integrated over a length L, the shear stress is a function of the pressure drop and the radial position, as shown in equation a12. Also shown is an expression for the wall stress.

$$\tau_{rz} = \frac{\Delta P}{2L}r \qquad \& \qquad \tau_\omega = \frac{\Delta P}{2L}R \tag{a12}$$

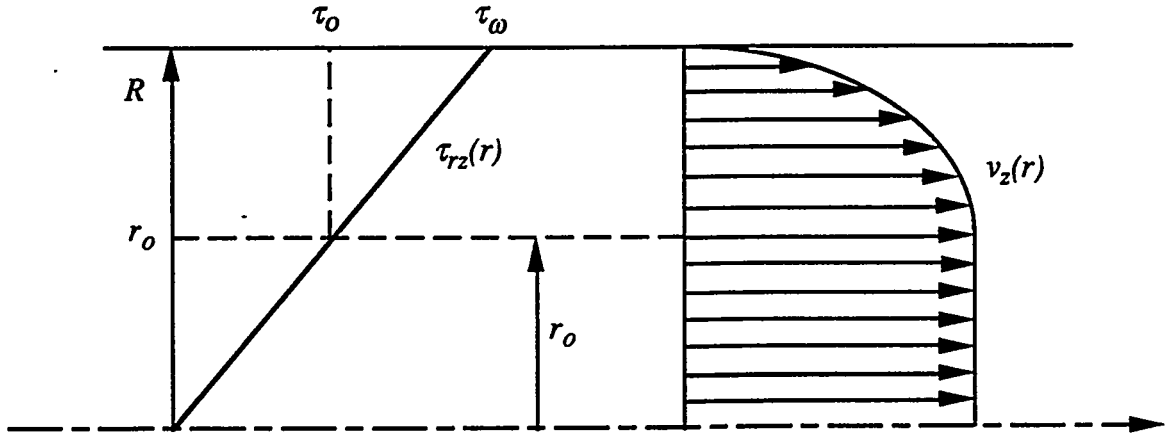

Figure A3: Radial shear stress and velocity distributions for fully-developed laminar flow of a yield/power law fluid.

Putting the shear stress in terms of the wall stress in the constitutive equation for a yield/power law fluid and rearranging, results in a first order ordinary differential equation for the axial velocity.

$$-\frac{dv_z}{dr}=\frac{1}{\eta_o^{1/n}}\left(\tau_\omega\frac{r}{R}-\tau_o\right)^{1/n} \tag{a13}$$

This equation is integrated directly, and the no-slip boundary condition is applied at the wall. Equation a15 is the velocity distribution for $r_O<r<R$. The uniform velocity for the inner region, where the shear stress is less than the yield stress, results from substituting r_O into equation a15. The result is equation a16.

$$v_z=-\frac{1}{\eta_o^{1/n}}\int\left(\tau_\omega\frac{r}{R}-\tau_o\right)^{1/n}dr=-\frac{nR}{(n+1)\tau_\omega\eta_o^{1/n}}\left(\tau_\omega\frac{r}{R}-\tau_o\right)^{\frac{n+1}{n}}+C \tag{a14}$$

$$v_{z_2}=\frac{nR}{(n+1)\tau_\omega\eta_o^{1/n}}\left[(\tau_\omega-\tau_o)^{\frac{n+1}{n}}-\left(\tau_\omega\frac{r}{R}-\tau_o\right)^{\frac{n+1}{n}}\right] \tag{a15}$$

$$v_{z_1}=\frac{nR}{(n+1)\tau_\omega\eta_o^{1/n}}\left[(\tau_\omega-\tau_o)^{\frac{n+1}{n}}-\left(\tau_\omega\frac{r_o}{R}-\tau_o\right)^{\frac{n+1}{n}}\right] \tag{a16}$$

Substituting equation a12 for the wall stress into equations a15 and a16 results in the velocity distribution in terms of the pipe length and pressure drop, generally, known quantities. Equations a17 and a18 are the expressions for the velocity distributions in the inner and outer regions of the flow.

$$v_{z_1}=\frac{2Ln}{(n+1)\Delta P\eta_o^{1/n}}\left(\frac{\Delta PR}{2L}-\tau_o\right)^{\frac{n+1}{n}} \qquad 0\le r\le r_o \tag{a17}$$

$$v_{z_2}=\frac{2Ln}{(n+1)\Delta P\eta_o^{1/n}}\left[\left(\frac{\Delta PR}{2L}-\tau_o\right)^{\frac{n+1}{n}}-\left(\frac{\Delta \mathrm{Pr}}{2L}-\tau_o\right)^{\frac{n+1}{n}}\right] \qquad r_o\le r\le R \tag{a18}$$

The volume flow rate is determined by integrating the velocity distribution over the the pipe cross-section area.

$$Q=\int_0^R v_z(r)2\pi r dr=2\pi\int_0^{r_o}v_{z_1}rdr+2\pi\int_{r_o}^R v_{z_2}rdr \tag{a19}$$

Carrying out the integration in equation a19 and substituting equation a20 for the threshold radius, r_O, results in an expression for the flow rate as a function of the pressure drop, pipe geometry, and the fluid rheological properties. With some manipulation, the resultant expression for the flow rate/pressure drop relationship for a yield/power law fluid is equation a21. This equation is analogous to the Buckingham-Reiner equation for a Bingham plastic, (Bird, Stewart, & Lightfoot, 1960).

$$r_o = \frac{R\tau_o}{\tau_\omega} = \frac{2L\tau_o}{\Delta P} \tag{a20}$$

$$Q = \frac{4\pi Ln}{(n+1)\Delta P \eta_o^{1/n}} \left\{ \frac{R^2}{2}\left(\frac{\Delta PR}{2L} - \tau_o\right)^{\frac{n+1}{n}} - \frac{4nL^2}{\Delta P^2}\left[\frac{\left(\frac{\Delta PR}{2L} - \tau_o\right)^{\frac{3n+1}{n}}}{3n+1} + \frac{\tau_o\left(\frac{\Delta PR}{2L} - \tau_o\right)^{\frac{2n+1}{n}}}{2n+1} \right] \right\} \tag{a21}$$

Setting the exponent n equal to one in equation a21 results in an expression for the flow rate/pressure drop relationship for a Bingham plastic, equation a22. This equation can be simplified, and the Buckingham-Reiner equation is recovered, equation a23. This exercise verifies that equation a21 is correct.

$$Q = \frac{4\pi L}{2\Delta P \eta_o} \left\{ \frac{R^2}{2}\left(\frac{\Delta PR}{2L} - \tau_o\right)^2 - \frac{4L^2}{\Delta P^2}\left[\frac{\left(\frac{\Delta PR}{2L} - \tau_o\right)^4}{4} + \frac{\tau_o\left(\frac{\Delta PR}{2L} - \tau_o\right)^3}{3} \right] \right\} \tag{a22}$$

$$Q = \frac{\pi \Delta PR^4}{8L\eta_o}\left[1 - \frac{8}{3}\frac{L\tau_o}{\Delta PR} + \frac{16}{3}\left(\frac{L\tau_o}{\Delta PR}\right)^4\right] \tag{a23}$$

This Page Intentionally Left Blank

Appendix B Dimensional Analysis of Pipe Flow of a Yield/Power Law Fluid

Dimensional analysis reduces the complexity of a problem by reducing the number of independent parameters to the minimum number of dimensionless parameters that are required to adequately describe the phenomena under investigation. For pipe flow of a yield/power law non-Newtonian fluid, dimensional analysis will give the correct forms of the Reynolds and Hedstrom numbers. These non-dimensional parameters will allow the laminar/turbulent flow transition for a yield/power law fluid to be treated in a similar manner to that of a Bingham fluid, (Hanks, 1963).

Buckingham's pi theorem is a dimensional analysis method that is commonly presented in elementary fluid mechanics texts. There are four sequential steps to the method, (Gerhart & Gross, 1985).

Step #1 *Write a functional expression for the dimensional relation under investigation.*

A functional relation for the frictional pressure drop of fully-developed laminar flow of a yield/power law fluid includes the fluid rheology, the pipe geometry, and the flow velocity. Equation b1 is the constituitive relation for a yield/power law fluid, and equation b2 is the functional expression for the pressure drop.

$$\tau_{rz} = \tau_o + \eta_o\left(-\frac{\partial v_z}{\partial r}\right)^n = \tau_o + \eta_o\dot{\gamma}^n \qquad \text{(b1)}$$

$$\Delta P = f(D, L, V, \rho, \eta_o, \tau_o) \qquad \text{(b2)}$$

The exponent n is not included in the functional relationship because it is a non-dimensional parameter.

Step #2 *Determine the number of dimensionless parameters you need to construct.*

The units of the dimensional parameters are as follows:

$$\Delta P = Pa = \frac{kg}{ms^2}$$

$$D = m$$

$$L = m$$

$$V = {}^{m}/_{s}$$

$$\rho = {}^{kg}/_{m^3}$$

$$\eta_o = \frac{kg}{ms^{2-n}}$$

$$\tau_o = \frac{kg}{ms^2}$$

There are three fundamental dimensions in this problem: length, mass, and time. The number of dimensionless parameters is equal to the number of dimensional parameters, z=7, minus the number of fundamental parameters, k=3. Four dimensionless parameters will be constructed.

$$z-k=7-3=4 \tag{b3}$$

Step #3 *Select k of the dimensional parameters that contain among them all of the fundamental dimensions. Combine these parameters with the remaining (z-k) dimensional parameters to form the required number, (z-k), of dimensionless parameters. This is done by selecting the remaining (z-k) parameters one at a time and multiplying by appropriate powers of the k repeating variables so that the result is dimensionless.*

The three dimensional parameters that contain all of the fundamental units and that will be used to form the four dimensionless parameters are the diameter, the velocity, and the density. These three repeating variables, taken to arbitrary powers, are sequentially multiplied by the remaining four variables. Equation b4 is the product of ΔP and the repeating variables.

$$\Pi_1 = \Delta P D^a V^b \rho^c \tag{b4}$$

The appropriate dimensions are substituted equation b4, and the exponents are combined. The pi term is non-dimensional when the exponents of the three fundamental dimensions are zero. Setting each of the three exponents, on the right side of equation b5, equal to zero results in three equations that are solved for the three exponents: a,b, and c.

$$\Pi_1 = \left(\frac{kg}{ms^2}\right)m^a\left(\frac{m}{s}\right)^b\left(\frac{kg}{m^3}\right)^c = kg^{1+c}m^{-1+a+b-3c}s^{-2-b} \tag{b5}$$

Substituting the values of the three exponents into the original pi term results in the dimensionless variable. Equation b6 is the expression for the dimensionless pressure drop.

$$\Pi_1 = \Delta P D^0 V^{-2} \rho^{-1} = \frac{\Delta P}{\rho V^2} \tag{b6}$$

The remaining three dimensionless variables are determined in the same manner.

$$\Pi_2 = L D^a V^b \rho^c \tag{b7}$$

$$\Pi_2 = m^1 m^a\left(\frac{m}{s}\right)^b\left(\frac{kg}{m^3}\right)^c = kg^c m^{1+a+b-3c}s^{-b-3c} \tag{b8}$$

$$\Pi_2 = L D^{-1} V^0 \rho^0 = \frac{L}{D} \tag{b9}$$

$$\Pi_3 = \eta_o D^a V^b \rho^c \tag{b10}$$

$$\Pi_3 = \left(\frac{kg}{ms^{2-n}}\right) m^a \left(\frac{m}{s}\right)^b \left(\frac{kg}{m^3}\right)^c = kg^{1+c} m^{-1+a+b-3c} s^{-(2-n)-b} \qquad \text{(b11)}$$

$$\Pi_3 = \eta_o D^{-n} V^{n-2} \rho^{-1} = \frac{\eta_o}{\rho V^{2-n} D^n} \qquad \text{(b12)}$$

$$\Pi_4 = \tau_o D^a V^b \rho^c \qquad \text{(b13)}$$

$$\Pi_4 = \left(\frac{kg}{ms^2}\right) m^a \left(\frac{m}{s}\right)^b \left(\frac{kg}{m^3}\right)^c = kg^{1+c} m^{-1+a+b-3c} s^{-2-b} \qquad \text{(b14)}$$

$$\Pi_4 = \tau_o D^0 V^{-2} \rho^{-1} = \frac{\tau_o}{\rho V^2} \qquad \text{(b15)}$$

Step #4 *Rearrange the Π groups to please yourself or to correspond with customary usage.*

Π_3 inverted is the Reynolds number for a yield/power law fluid. Multiplying Π_4 by the square of the Reynolds number results in the Hedstrom number. These are the two important non-dimensional parameters that govern pipe flow of a non-Newtonian fluid.

$$\mathrm{Re} = \frac{\rho V^{2-n} D^n}{\eta_o} \qquad \text{(b16)}$$

$$He = \left(\frac{\tau_o}{\rho V^2}\right)\left(\frac{\rho V^{2-n} D^n}{\eta_o}\right)^2 = \frac{\rho \tau_o D^{2n} V^{2(1-n)}}{\eta_o^2} \qquad \text{(b17)}$$

These two parameters differ from the analogous non-dimensional parameters for a Bingham fluid by the presence of the exponents involving *n*. If *n* is set to a value of one, the Reynolds and Hedstrom numbers for a Bingham plastic result. Equation b18 is the non-dimensional functional form that is equivalent to the dimensional expression, equation b2.

$$\frac{\Delta P}{\rho V^2} = F\left(\frac{L}{D}, \frac{\rho V^{2-n} D^n}{\eta_o}, \frac{\rho \tau_o D^{2n} V^{2(1-n)}}{\eta_o^2}\right) \qquad \text{(b18)}$$

This Page Intentionally Left Blank

Appendix C Laminar-Turbulent Transition for Flow of a Yield/Power Law Fluid in a Pipe

The transition Reynolds number for laminar to turbulent flow of a non-Newtonian fluid is not a constant but a function of the fluid properties and the pipe diameter. (Hanks, 1963) developed a general criterion for the stability threshold of a laminar velocity profile, based on the local ratio of the acceleration force to the viscous force. Equation c1 is the appropriate form of the stability threshold criterion for pipe flow. Based on an analysis of laminar flow of Newtonian fluids, the maximum value of K at transition was determined to be 404, and this value should apply to all non-thixotropic fluids.

$$K = \frac{1}{2}\frac{\rho}{dp/dz}\frac{d}{dr}\left(v^2\right) \qquad \text{(c1)}$$

(Hanks, 1963) used this criterion to derive expressions for the transition Reynolds numbers for Bingham plastics and Powell-Eyring fluids, and he demonstrated good agreement between theory and data. In this appendix, (Hanks, 1963) procedure is applied to a yield/power law fluid, equation c2, and a relation for the transition Reynolds number is derived.

$$\tau_{rz} = \tau_o + \eta_o\left(-\frac{\partial v_z}{\partial r}\right)^n = \tau_o + \eta_o\dot{\gamma}^n \qquad \text{(c2)}$$

The parameter K is zero at the centerline and the wall, and positive elsewhere. When the maximum value of K reaches 404, the flow will start to transition from laminar to turbulent flow, and the Reynolds number of the flow is the transition Reynolds number. In principle this procedure can be applied to any flow for which an analytical expression for the velocity profile exists.

Equations c3 and c4 are the expressions for the velocity profile of steady laminar fully-developed pipe flow of a yield power law fluid. For the pipe geometry, refer to figure A4, and the two following equations are equations a14 and a15 respectively.

$$v_z = \frac{nR}{(n+1)\tau_\omega \eta_o^{1/n}}\left[\left(\tau_\omega - \tau_o\right)^{\frac{n+1}{n}} - \left(\tau_\omega\frac{r}{R} - \tau_o\right)^{\frac{n+1}{n}}\right] \qquad r_o \le r \le R \qquad \text{(c3)}$$

$$v_z = \frac{nR}{(n+1)\tau_\omega \eta_o^{1/n}}\left[\left(\tau_\omega - \tau_o\right)^{\frac{n+1}{n}} - \left(\tau_\omega\frac{r_o}{R} - \tau_o\right)^{\frac{n+1}{n}}\right] \qquad 0 \le r \le r_o \qquad \text{(c4)}$$

The radial coordinate and the radius of the plastic plug are rendered dimensionless by the following expressions, and equations c5 and c6 are the resultant expressions for the velocity profile.

$$\xi = \frac{r}{R} \qquad \alpha = \frac{r_o}{R} = \frac{\tau_o}{\tau_\omega}$$

$$v_1 = \frac{nR\tau_\omega^{1/n}}{(n+1)\eta_o^{1/n}}(1-\alpha)^{\frac{n+1}{n}} \qquad 0 \le \xi \le \alpha \qquad \text{(c5)}$$

$$v_2 = \frac{nR\tau_\omega^{1/n}}{(n+1)\eta_o^{1/n}}\left[(1-\alpha)^{\frac{n+1}{n}} - (\xi-\alpha)^{\frac{n+1}{n}}\right] \qquad \alpha \le \xi \le 1 \qquad \text{(c6)}$$

The mean velocity is calculated by integrating the velocity profile as shown in equation c7. Equation c8 is the expression for the mean velocity.

$$\bar{v} = \frac{1}{\pi R^2}\int_0^R v(r)2\pi r dr = 2\int_0^1 v(\xi)\xi d\xi \qquad \text{(c7)}$$

$$\bar{v} = \frac{2nR\tau_\omega^{1/n}}{(n+1)\eta_o^{1/n}}\left[\frac{1}{2}(1-\alpha)^{\frac{n+1}{n}} - \frac{n\alpha(1-\alpha)^{\frac{2n+1}{n}}}{2n+1} - \frac{n(1-\alpha)^{\frac{3n+1}{n}}}{3n+1}\right] \qquad \text{(c8)}$$

Equation c9 is the appropriate form for the Reynolds number for a yield/power law fluid, see Appendix B. Substituting equation c8, the expression for the mean velocity, into the definition for the Reynolds number and expressing the wall shear stress in terms of the yield stress results in equation c10, the expression for the Reynolds number as a function of α. If the critical value of α, where transition from laminar to turbulent flow occurs, can be calculated, the transition Reynolds number can be determined with equation c10.

$$\mathrm{Re} = \frac{\rho\bar{v}^{2-n}D^n}{\eta_o} = \frac{2^n\rho\bar{v}^{2-n}R^n}{\eta_o} \qquad \text{(c9)}$$

$$\mathrm{Re} = \frac{4n^{2-n}\rho R^2\tau_o^{\frac{2-n}{n}}}{(n+1)^{2-n}\eta_o^{2/n}\alpha^{\frac{2-n}{n}}}\left[\frac{1}{2}(1-\alpha)^{\frac{n+1}{n}} - \frac{n\alpha(1-\alpha)^{\frac{2n+1}{n}}}{2n+1} - \frac{n(1-\alpha)^{\frac{3n+1}{n}}}{3n+1}\right]^{2-n} \qquad \text{(c10)}$$

The expression for the parameter K, equation c1, for a yield/power law fluid is determined by expressing the axial pressure gradient in terms of the wall shear stress, equation c11, and substituting in the velocity profile expression. Equation c13 is the expression for this parameter.

$$\tau_\omega = -\frac{dP}{dz}\frac{R}{2} \qquad \text{(c11)}$$

$$K = \frac{1}{2}\frac{\rho}{dP/dz}\frac{d}{dr}\left(v^2\right) = -\frac{\rho}{2\tau_\omega}v\frac{dv}{d\xi} \qquad \text{(c12)}$$

$$K = \frac{n\rho\tau_\omega^{\frac{2-n}{n}}R^2}{2(n+1)\eta_o^{2/n}}\left[(1-\alpha)^{\frac{n+1}{n}}(\xi-\alpha)^{1/n} - (\xi-\alpha)^{\frac{n+2}{n}}\right] \qquad \text{(c13)}$$

Equation c13 is differentiated and set equal to zero in order to determine the radial position where K is a maximum. The radial position where K is a maximum is determined by the appropriate root of equation c16.

$$\frac{dK}{d\xi} = \frac{\rho \tau_\omega^{\frac{2-n}{n}} R^2}{2(n+1)\eta_o^{2/n}} \left[(1-\alpha)^{\frac{n+1}{n}} (\xi-\alpha)^{\frac{1-n}{n}} - (n+2)(\xi-\alpha)^{2/n} \right] \tag{c14}$$

$$\frac{dK}{d\bar{\xi}} = 0 \tag{c15}$$

$$(1-\alpha)^{\frac{n+1}{n}} \left(\bar{\xi}-\alpha\right)^{\frac{1-n}{n}} - (n+2)\left(\bar{\xi}-\alpha\right)^{2/n} = 0 \tag{c16}$$

Equation c17 is the expression for the radial position where K is a maximum. The transition to turbulence starts at the point where the maximum value of K is equal to 404. Equation c17 is substituted into equation c13, and the parameter K is set equal to 404. This is equation c19. This expression relates the critical value of α, the radial position where the velocity profile becomes unstable, to fluid properties. Equation c20 is the expression for α_c, the critical value of α, as a function of the fluid properties and the pipe radius. The value of α_c is substituted into equation c10 to determine the transition Reynolds number.

$$\bar{\xi} = \alpha + \frac{1-\alpha}{(n+2)^{\frac{n}{n+1}}} \tag{c17}$$

$$K\left(\bar{\xi}\right)_{trans.} = 404 \tag{c18}$$

$$404 = \frac{n\rho \tau_o^{\frac{2-n}{n}} R^2}{2\eta_o^{2/n} \alpha_c^{\frac{2-n}{n}}} \left[\frac{(1-\alpha_c)^{\frac{n+2}{n}}}{(n+2)^{\frac{n+2}{n+1}}} \right] \tag{c19}$$

$$\frac{\alpha_c}{(1-\alpha_c)^{\frac{n+2}{2-n}}} = \frac{\rho^{\frac{n}{2-n}} \tau_o R^{\frac{2n}{2-n}}}{\eta_o^{\frac{2}{2-n}}} \left[\frac{n}{808(n+2)^{\frac{n+2}{n+1}}} \right]^{\frac{n}{2-n}} \tag{c20}$$

Equation c19 can be used to simplify equation c10, the expression for the transition Reynolds number. Equation c19 is manipulated into the form shown in equation c21. The left side of this equation is the grouping of the fluid properties in equation c10. Substituting equation c21 into equation c10, results in an expression for the transition Reynolds number as a function of α_c and n.

$$\frac{\rho R^2 \tau_o^{\frac{2-n}{n}}}{\eta_o^{2/n} \alpha_c^{\frac{2-n}{n}}} = \frac{2(404)(n+2)^{\frac{n+2}{n+1}}}{n(1-\alpha_c)^{\frac{n+2}{n}}} \tag{c21}$$

$$\mathrm{Re}_c = \frac{3232 n^{1-n}(n+2)^{\frac{n+2}{n+1}}}{(n+1)^{2-n}(1-\alpha_c)^{\frac{n+2}{n}}}\left[\frac{1}{2}(1-\alpha_c)^{\frac{n+1}{n}} - \frac{n\alpha_c(1-\alpha_c)^{\frac{2n+1}{n}}}{2n+1} - \frac{n(1-\alpha_c)^{\frac{3n+1}{n}}}{3n+1}\right]^{2-n} \qquad \text{(c21)}$$